Biosensors and Bioelectronics 66 (2015) 350–355

Contents lists available at ScienceDirect

Biosensors and Bioelectronics

journal homepage: www.elsevier.com/locate/bios

Biosensor based on glucose oxidase-nanoporous gold co-catalysis for glucose detection

Chao Wu, Huihui Sun, Yufei Li, Xueying Liu, Xiaoyu Du, Xia Wang *, Ping Xu [1]

State Key Laboratory of Microbial Technology, Shandong University, Jinan 250100, PR China

ARTICLE INFO

Article history:
Received 14 August 2014
Received in revised form
18 November 2014
Accepted 20 November 2014
Available online 24 November 2014

Keywords:
Glucose oxidase
Immobilization
Nanoporous gold
Biosensor
Glucose

ABSTRACT

Promoting the electrocatalytic oxidation of glucose is crucial in glucose biosensor design. In this study, nanoporous gold (NPG) was selected for glucose oxidase (GOx) immobilization and glucose biosensor fabrication because of its open, highly conductive, biocompatible, and interconnected porous structure, which also facilitates the electrocatalytic oxidation of glucose. The electrochemical reaction on the surface of the resulting GOx/NPG/GCE bioelectrode was attributed to the co-catalysis effect of GOx and NPG. A surface-confined reaction in a phosphate buffer solution was observed at the bioelectrode during cyclic voltammetry experiments. Linear responses were observed for large glucose concentrations ranging from 50 μM to 10 mM, with a high sensitivity of 12.1 μA mM^{-1} cm^{-2} and a low detection limit of 1.02 μM. Furthermore, the GOx/NPG/GCE bioelectrode presented strong anti-interference capability against cholesterol, urea, tributyrin, ascorbic acid, and uric acid, along with a long shelf-life. For the detection of glucose in human serum, the data generated by the GOx/NPG/GCE bioelectrode were in good agreement with those produced by an automatic biochemical analyzer. These unique properties make the GOx/NPG/GCE bioelectrode an excellent choice for the construction of a glucose biosensor.

1. Introduction

Glucose plays a crucial role in life processes (Heller and Feldman, 2008) as a direct energy source facilitating various biological activities. More specifically, the serum glucose is a clinically significant indicator of many chronic illnesses such as diabetes, obesity, hyperglycemia, and cardiovascular disease (Jiang et al., 2008; Wei et al., 2014). Therefore, it is highly desirable to develop a new method for the rapid and efficient determination of blood glucose.

As compared to the traditional methods available for glucose detection, methods based on electrochemical sensors show unique advantages such as high selectivity and sensitivity, ease of operation, fast response, and continuous real-time detection (Gu et al., 2012). Nonenzymatic electrochemical sensors have been widely used for glucose determination because of their high stability and operational simplicity (Chang et al., 2014; Fu et al., 2014). However, the selectivity and sensitivity of nonenzymatic sensors are usually inferior to those of the biosensors incorporating enzymes as the recognition elements. In 1962, Clark and Lyons (1962) developed the first biosensor system comprising glucose oxidase (GOx) coupled with an oxygen electrode. Since then, GOx has been widely used in biosensors to determine the glucose levels in serum sample in vitro (Qiu et al., 2012; Gao et al., 2014; Hsu and Wang, 2014). However, the inherent characteristics of enzymes are considered a mixed blessing, because efficient catalysis is often accompanied by a higher possibility of enzyme inactivation. Thus, the materials that link the enzymes to the electrode need to conserve the enzymatic activity by providing an efficient electron transfer and by achieving sufficient enzyme loading. However, research aimed at using inorganic materials for enzyme immobilization has been rarely carried out. Such immobilization could potentially facilitate the simultaneous electrocatalytic activities of the enzyme and the inorganic material towards the substrate.

In recent years, various nanomaterials were employed as enzyme immobilization substrates and as recognition elements in electrochemical sensors. High biosensor performance, intimate enzyme attachment, and effective electron transfer are achievable because of the high surface area, and the unique physical, electronic, and chemical properties of nanomaterials (Vijayalakshmi et al., 2008; Solanki et al., 2009). Among the various nanomaterials, nanoporous gold (NPG) has attracted much attention in the fabrication of nonenzymatic and enzyme-based electrochemical sensors because of its excellent structural continuity, higher conductivity, and general biocompatibility (Ding et al., 2004; Ding and

* Corresponding author. Fax: +86 531 88366231.
E-mail address: ghwx@sdu.edu.cn (X. Wang).
[1] Present address: Key Laboratory of Microbial Metabolism and School of Life Sciences and Biotechnology, Shanghai Jiao Tong University, Shanghai 200240, PR China.

http://dx.doi.org/10.1016/j.bios.2014.11.037
0956-5663/

Chen, 2009; Scanlon et al., 2012; Yan et al., 2012; Zhang and Ding, 2013). The active surface and catalytic activity of NPG also provides us with the possibility of substrate recognition even in the absence of the enzyme. For example, hydrogen peroxide and glucose elicited a direct electrochemical response form a nonenzymatic NPG sensor (El-Daeb and Ohsaka, 2002; Liu et al., 2009). While NPG also provides a natural platform for stable enzyme immobilization because of the strong gold–sulfur covalent-type interactions, enzyme/NPG biocomposites are expected to combine the advantages of both enzymatic and nonenzymatic electrochemical sensors, and exhibit a synergistic effect that results into highly efficient glucose detection.

In our previous work, enzyme/NPG biocomposites were successfully constructed by assembling various enzymes (such as lipase, catalase, and horseradish peroxidase) onto NPG (Wang et al., 2011). A lipase/NPG biosensor was also reported to perform exceptionally well during the detection of serum triglycerides (TGs) (Wu et al., 2014). This study was devoted to confirming whether GOx and NPG could offer a synergistic electrocatalytic effect towards glucose. We also focused on the construction of a GOx/NPG co-catalytic biosensor for glucose detection. The resulting GOx/NPG/GCE bioelectrode seems to exhibit excellent sensitivity, selectivity, and stability, along with a good anti-interference ability and repeatability

2. Experimental

2.1. Chemicals

GOx (Sigma G7141 from *Aspergillus niger*; protein: 65–85%; molecular weight: 160 kDa) was purchased from Sigma-Aldrich (St. Louis, MO, USA). D-Glucose (analytical grade) was purchased from Shanghai Sangon Biotech Co. LTD (China). All other chemicals used were of analytical grade.

D-Glucose was dissolved in a PBS (50 mM, pH 7.0) solution to form a 2 M glucose stock solution. The glucose stock solution was stored in a refrigerator at 4 °C in the dark.

2.2. Preparation of the NPG/GCE electrode

NPG was made by dealloying 12-carat white gold leaves (Au50Ag50 wt%, Sepp Leaf Products, USA) in concentrated HNO_3 at 30 °C for 30 min. After that, NPG was washed with ultrapure water until the pH to 7.0. It was then kept in ultrapure water.

Glassy carbon electrodes (GCEs) were polished with a 0.05 μm alumina slurry on a piece of chamois leather. Before use, the GCEs were cleaned ultrasonically in the mixture of HNO_3 and water mixed in a 1:1 ratio (v/v), and washed with ultrapure water and absolute ethanol, respectively. The GCE was then coated with an NPG leaf in ultrapure water to form NPG/GCE. The NPG/GCE was placed in a vacuum drier for later use.

2.3. GOx immobilization

GOx solution (2000 U mL^{-1}) was freshly prepared by dissolving 34 mg GOx in 5 mL PBS (50 mM, pH 6.8) prior to being used. One unit (U) of GOx activity is defined as the amount of GOx, which oxidizes 1.0 μM of β-D-glucose to D-gluconolactone and H_2O_2 per min at pH 5.1, at 35 °C. The freshly prepared NPG/GCE was immersed immediately into the GOx solution. After a 72 h immobilization, the GOx/NPG/GCE bioelectrode was immersed into the PBS solution (50 mM, pH 7.0) and then transferred to a refrigerator (4 °C) for subsequent use.

2.4. Measurement

The morphology of NPG was characterized using a Nova NanoSEM 450 field emission scanning electron microscope (SEM) equipped with an energy-dispersive X-ray spectrometer (EDS).

All the electrochemical measurements were performed in a conventional three-electrode cell at room temperature. The cyclic voltammograms (CVs) and linear sweep voltammograms (LSVs) were measured using a three-electrode conventional cell with a CHI 760D electrochemical workstation (Shanghai Chenhua Apparatus Corporation, China). The modified GCE was used as a working electrode, and a Pt sheet (1 cm × 1 cm) and a saturated calomel electrode (SCE) were used as counter and reference electrodes, respectively. All the potentials were referred to the SCE. The electrolyte solutions were deaerated by N_2 bubbling for 10 min prior to the electrochemical measurements, and a blanket of N_2 was maintained throughout each experiment.

2.5. Detection of GOx concentration in serum

Serum samples were offered by a school hospital affiliated to the Shandong University (Jinan, China). The serum sample (500 μL) was added to 15 mL deaerated PBS (50 mM, pH 7.0) in a three-electrode system, with the GOx/NPG/GCE as the working electrode. In order to validate the values measured by the GOx/NPG/GCE electrode, the serum samples were also analyzed with an automatic biochemical analyzer (HITACHI 7100, Japan).

3. Results and discussion

3.1. Construction and characterization of the GOx/NPG/GCE bioelectrode

The dimensions of GOx, as revealed by its crystal structure were 7 × 5.5 × 8.0 cubic nm (Hecht and Schomburg, 1993). According to theoretical calculations, the maximum stabilization of a protein can be achieved following adsorption within spherical cages whose diameter are 2–6 times those of the native molecule (Sotiropoulou et al., 2005; Wang et al., 2011). Therefore, NPG with a pore size of ca. 35 nm, was selected to link GOx for constructing the GOx/NPG/GCE bioelectrode depicted in Fig. 1. The samples before (Fig. 1A) and after (Fig. 1B) GOx loading were characterized using SEM. Fig. 1A illustrates an open three-dimensional nanoporous structure. The EDS compositional analysis reveals that only Au was detected, thus indicating that the residual Ag was below the detection limit of about 0.5% (Fig. 1C). A preferential immobilization of GOx over the ligament site with high radial curvatures was achieved, as evident from the smaller pore size and coarser surface morphology of the GOx/NPG biocomposite (Fig. 1B), relative to the bare NPG (Fig. 1A). Additionally, the EDS analysis confirmed the existence of dominant elements such as C, N, and O (Fig. 1D), thus providing the primary evidence for a successful GOx immobilization onto NPG.

3.2. Electrochemical behavior of the GOx/NPG/GCE bioelectrode

The electrochemical behaviors of the NPG/GCE electrode and the GOx/NPG/GCE bioelectrode were compared in deaerated PBS (50 mM, pH 7.0) at a scan rate of 50 mV s^{-1}. The current response of the GOx/NPG/GCE electrode was obviously reduced, relative to the NPG/GCE bioelectrode, as shown in Fig. 2A. Because of the insulating character of the enzyme, the lower current response after GOx loading indicated that GOx was successfully immobilized onto NPG (Zhang et al., 2005; Qiu et al., 2012).

To confirm the functioning of the GOx/NPG/GCE bioelectrode

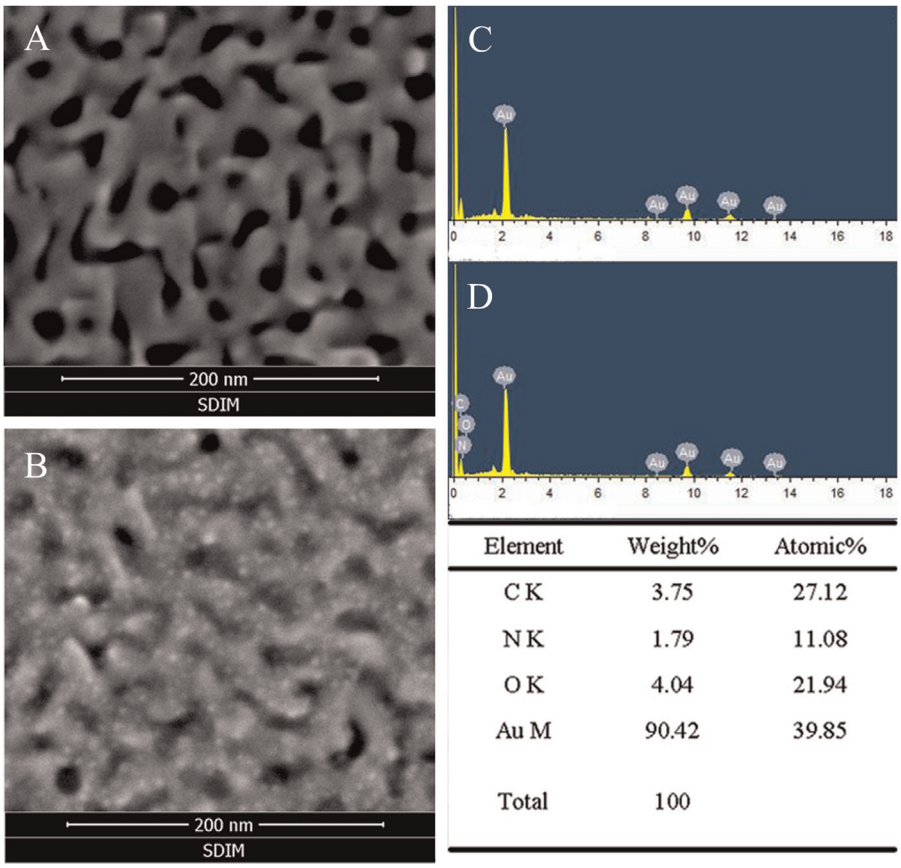

Element	Weight%	Atomic%
C K	3.75	27.12
N K	1.79	11.08
O K	4.04	21.94
Au M	90.42	39.85
Total	100	

Fig. 1. SEM images of NPG with a pore size of 35 nm before (A) and after the lipase loading (B); along with the corresponding EDS spectra (C and D).

during the electrocatalytic oxidation of glucose, the NPG/GCE electrode and GOx/NPG/GCE bioelectrode were compared in deaerated PBS (50 mM, pH 7.0) in the presence of 6 mM glucose at a scan rate of 50 mV s^{-1} as shown in Fig. 2B. The potential ranged from −0.7 to +1.2 V, and it included the NPG redox peaks, thus indicating the generation of Au surface oxides (Liu et al., 2009). Fig. 2B shows that both NPG/GCE and GOx/NPG/GCE showed electrocatalytic activity during glucose oxidation. According to Liu et al. (2009), the electrocatalytic oxidation of glucose by NPG/GCE electrode in the absence of GOx proceeds via the following reaction pathways:

$$Au+OH^- \rightarrow AuOH + e^- \quad (1)$$

$$C_5H_{10}O_5CHOH + AuOH \rightarrow C_5H_{10}O_5CHOAu + H_2O \quad (2)$$

$$C_5H_{10}O_5CHOAu \rightarrow C_5H_{10}O_5CO+Au + e^- +H^+ \quad (3)$$

The reaction process starts by adsorbing OH^-, via the adsorption of glucose onto the AuOH sites, thereby generating gluconolactone. A higher peak current density of the GOx/NPG/GCE bioelectrode was observed at +0.3 V as compared to that of the NPG/GCE electrode because of the efficient catalysis of GOx, thus indicating a better catalytic activity towards glucose than that of the nonenzymatic NPG/GCE at a low potential range (Fig. 2B). Upon GOx loading, the encapsulated enzyme occupied parts of the active sites of NPG, as evidenced by a slightly decreased current density in Fig. 2A. However, we did not see a significant current decrease in the glucose solution over the entire potential range from −0.7 to +1.2 V, thus indicating that covering GOx on NPG did not affect the glucose sensing at a high potential range of +0.8 to +1.2 V. Further examination was carried out to confirm the interaction of GOx with NPG by sweeping the CVs of the GOx/NPG/GCE bioelectrode and the NPG/GCE electrode from −0.7 to +0.5 V. Within this range, the NPG was not activated, thus indicating no electrochemical catalytic activity toward glucose. As shown in Fig. 3A, the redox reaction of GOx caused a new oxidation peak at +0.4 V, and a reduction peak at +0.3 V in deaerated PBS (50 mM, pH 7.0) in the absence of glucose. Once again, this indicated that the electrochemically active GOx was successfully immobilized onto NPG. These results were in accordance with the previous reports that well-defined redox peaks appeared after GOx was immobilized on nanostructured Au (Qiu et al., 2012). In comparison, no peaks were observed under the same conditions for the NPG/GCE electrode. When 10 mM glucose was added, an oxidation peak at +0.4 V in the positive going sweeps and a sharp oxidation peak at +0.3 V in the negative going sweeps occurred for the GOx/NPG/GCE bioelectrode. In contrast, no peaks were observed for the NPG/GCE electrode, as shown in Fig. 3B. These results indicated that NPG was not involved directly in the oxidation of glucose in the potential range from −0.7 to +0.5 V, and that the oxidation of glucose was solely catalyzed by GOx. In this case, the working principle of the GOx/NPG/GCE bioelectrode during the electrocatalytic oxidation of glucose could be expressed as follows:

$$C_6H_{12}O_6 + O_2 + H_2O \xrightarrow{GOx} C_6H_{12}O_7 + H_2O_2 \quad (4)$$

$$H_2O_2 + 2H^+ + 2e^- \xrightarrow{NPG} 2H_2O \quad (5)$$

In this way, GOx catalyzed the oxidation of glucose to gluconic acid, and NPG catalyzed the reduction of H_2O_2 to H_2O (Qiu et al., 2012; El-Daeb and Ohsaka, 2002). Additionally, GOx catalyzed the electrocatalytic oxidation of glucose at the same potential as that of NPG (+0.3 V), making GOx and NPG capable of oxidizing glucose at the same time in a wide potential range from −0.7 to

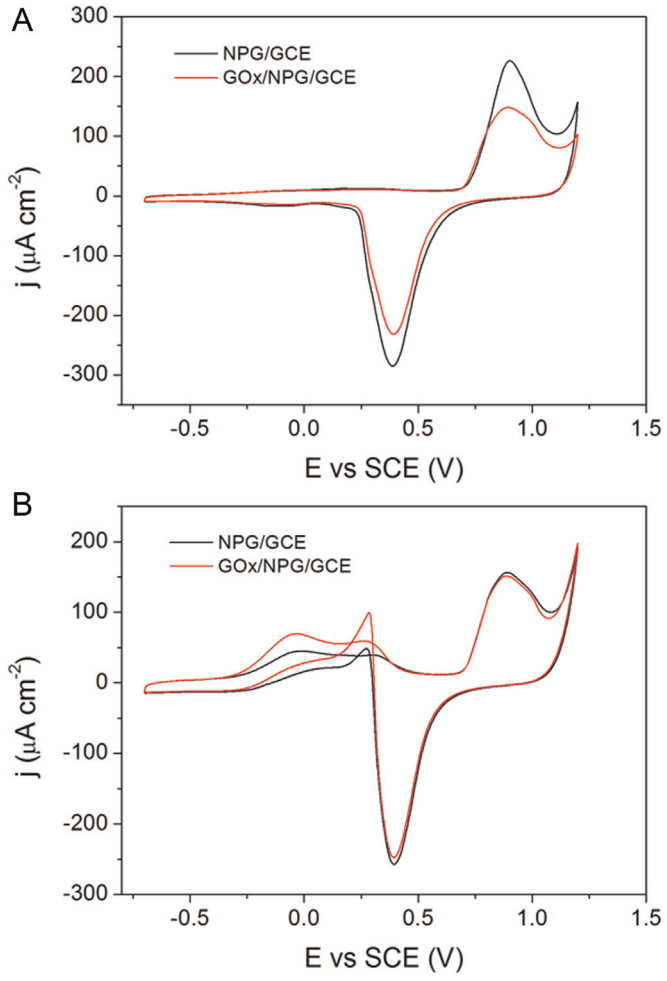

Fig. 2. CVs of the NPG/GCE electrode and the GOx/NPG/GCE bioelectrode in (A) PBS (50 mM, pH 7.0) and (B) PBS (50 mM, pH 7.0) with 6 mM glucose at a scan rate of 50 mV s^{-1}.

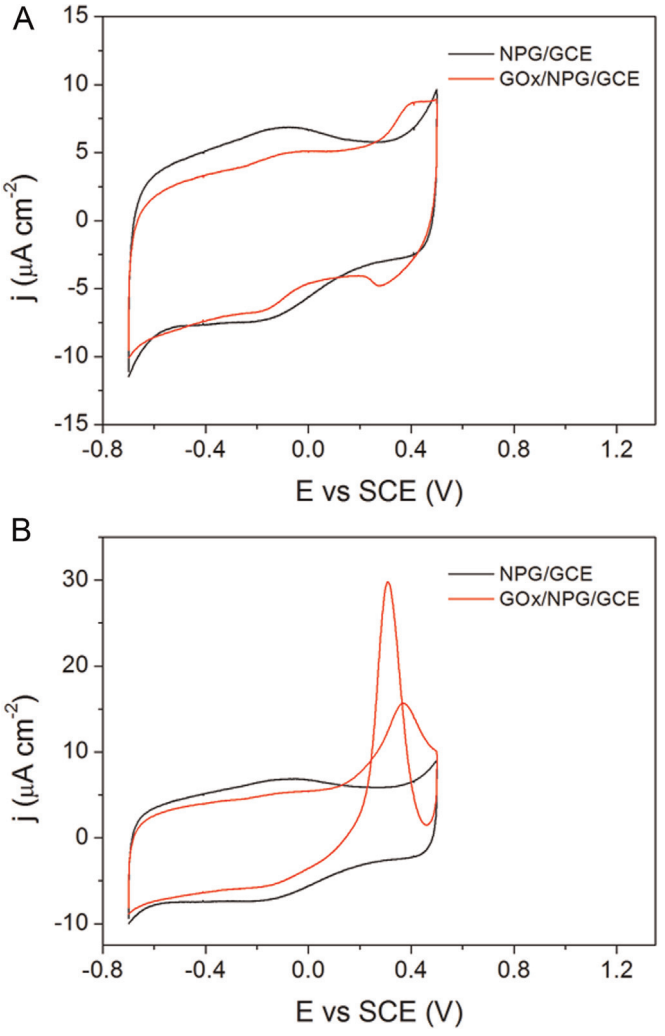

Fig. 3. CVs of the NPG/GCE electrode and the GOx/NPG/GCE bioelectrode in (A) PBS (50 mM, pH 7.0) and (B) PBS (50 mM, pH 7.0) with 10 mM glucose at a scan rate of 50 mV s^{-1}.

+1.2 V. Therefore, the higher current density of GOx/NPG/GCE at +0.3 V shown in Fig. 2B could be the result of enhanced electrochemical oxidation due to the synergistic effect of GOx and NPG effect towards glucose. Based on the above results, the electrochemical reaction on the surface of the GOx/NPG/GCE bioelectrode was attributed to the co-catalysis of GOx and NPG, as shown in Scheme 1. Such co-catalysis offered a better current response than that of GOx or NPG alone. Therefore, glucose detection was achieved by detecting the changes of the oxidation peak current density at a potential of 0.3 V in the negative going sweeps using the GOx/NPG/GCE bioelectrode.

Fig. 4A shows a group of CVs for the GOx/NPG/GCE bioelectrode at different scan rates in deaerated PBS (50 mM, pH 7.0). Obviously, the redox peak current density was dependent on the scan rate. As shown in the inset of Fig. 4A, a perfect linear relationship between the peak current density and the scan rate from 10 to 1000 mV s^{-1} was obtained by plotting the peak current density against the scan rate. The regression coefficients for the cathodic and anodic peaks were both 0.999, and the ratio of the cathodic peak current density to the anodic peak current density was approximately equal to 1. These typical characteristics confirmed that the electron transfer process was indeed a surface-controlled process (Qiu et al., 2012).

To characterize the quality of the GOx/NPG/GCE bioelectrode, the surface concentration of GOx on the NPG/GCE was calculated.

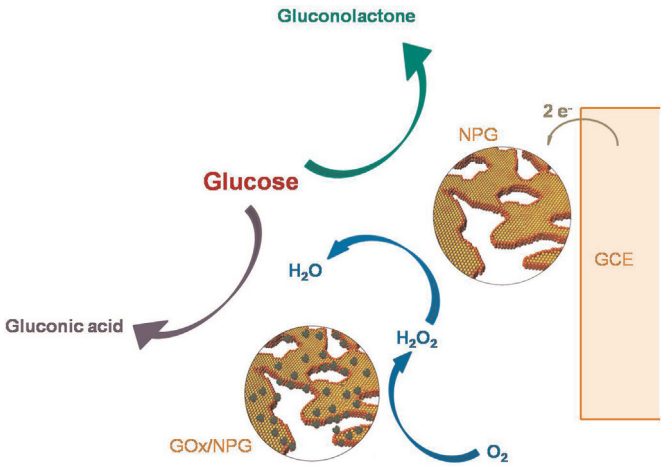

Scheme 1. Electrochemical reaction on the surface of the GOx/NPG/GCE bioelectrode.

The loading amount of GOx on NPG could be investigated using a voltammetric method adopted by Laviron (1979). The peak current density could be expressed as mentioned in Eq. (6) below

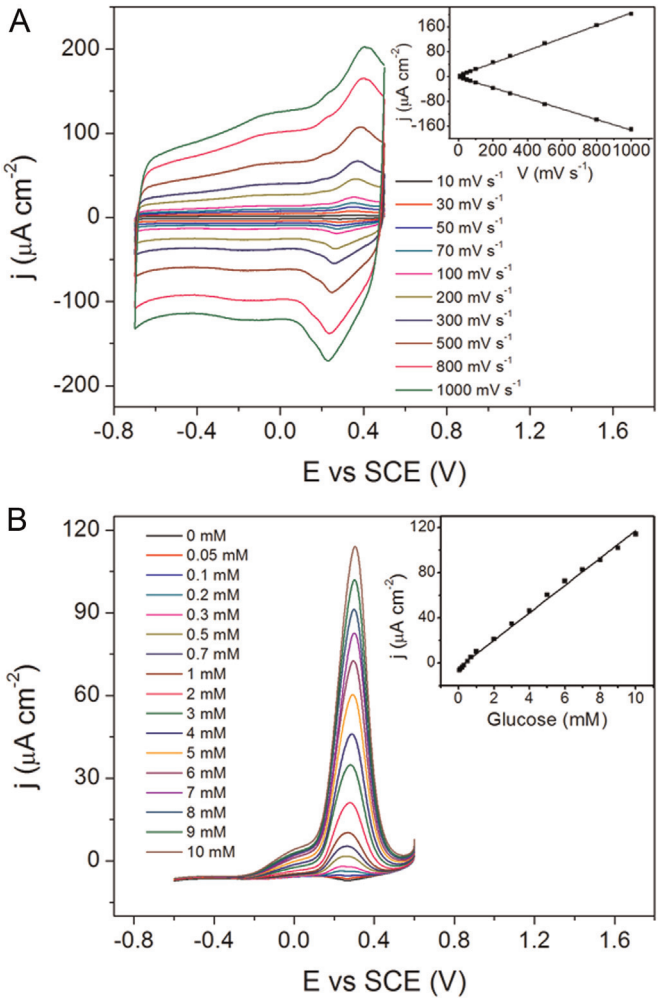

Fig. 4. Graphics of the GOx/NPG/GCE bioelectrode under different conditions. (A) CVs of the GOx/NPG/GCE bioelectrode at different scan rates ranging from 10 to 1000 mV s^{-1}. The inset profiles show the peak current density as a function of the scan rate. (B) electrochemical response of the GOx/NPG/GCE bioelectrode as a function of the glucose concentration. The inset profiles show the calibration curve between the peak current density and the glucose concentration (50 μM–10 mM).

$$I_p = \frac{nFQv}{4RT} = \frac{n^2F^2vA\Gamma^*}{4RT} \quad (6)$$

where n is the number of electrons transferred (2), I_p is the anodic peak current, A is the surface area (0.071 cm^2), Γ^* is the average surface concentration of GOx, ν is the scan rate, and T, R, and F are absolute temperature, ideal gas constant, and Faraday constant, respectively. According to Eq. (6), the average surface concentration of GOx immobilized onto the NPG/GCE is calculated to be 3.15×10^{-10} mol cm^{-2} from the slope of the I_p–ν curve. This value is higher than the value previously reported (2.58×10^{-10} mol cm^{-2}) for GOx immobilized on nanostructured Au thin films (Qiu et al., 2012). This result can be ascribed to the three-dimensional nanoporous structure of NPG, which facilitates the efficient immobilization of GOx.

3.3. Amperometric detection of glucose

The electrochemical response of GOx/NPG/GCE was investigated as a function of the glucose concentrations (50 μM–10 mM) using the LSV technique at a 50 mV s^{-1} scan rate in deaerated PBS (50 mM, pH 7.0). As shown in Fig. 4B, while the glucose concentration increased, the oxidation peak current density of the GOx/NPG/GCE bioelectrode also increased at the potential of +0.3 V. Moreover, the peak current densities were all proportional to the glucose concentration in a large range (50 μM–10 mM), with a correlation coefficient of 0.996. The GOx/NPG/GCE bioelectrode showed a high sensitivity of 12.1 μA mM^{-1} cm^{-2} and a low detection limit of 1.02 μM. These results indicated that the GOx/NPG/GCE bioelectrode possessed a larger linear range, higher sensitivity, and lower detection limit than most enzymatic or nonenzymatic glucose sensors, as shown in Table S1 (Supplementary information).

3.4. Stability and reproducibility of the GOx/NPG/GCE bioelectrode

Stability is a basic requirement for each biosensor. To investigate the stability of the GOx/NPG/GCE bioelectrode, it was preserved in ultrapure water at 4 °C. After a 28 day storage, the GOx/NPG/GCE bioelectrode retained 99.6% of its initial current response. Even after 42 days, 94.7% of its initial current response was retained by the GOx/NPG/GCE bioelectrode. These results confirmed that the GOx/NPG/GCE bioelectrode presented good stability because of a greater biocompatibility and because of the rarely inactivating catalytic sites provided by NPG (Ravindra et al., 2004; Sotiropoulou et al., 2005; Hudson et al., 2008; Wang et al., 2011; Wu et al., 2014). To investigate the reproducibility of the GOx/NPG/GCE bioelectrode, five consecutive measurements were recorded by detecting the current response of the GOx/NPG/GCE bioelectrode in the presence of 6 mM glucose, and the relative standard deviations (RSD) were 2.26%. The low RSD indicated that the biosensor exhibited good reproducibility.

3.5. Specificity and interference

The selectivity of the enzyme electrode is an important characteristic for the specific recognition of the target substrate. During this study, 10 mM cholesterol (Chol), 2 mM urea, 3.3 mM tributyrin (TB), 50 μM ascorbic acid (AA), and 0.2 mM uric acid (UA) were added into the deaerated PBS (50 mM, pH 7.0) containing 6 mM glucose to evaluate the specificity of the GOx/NPG/GCE bioelectrode. The amounts of the added interferents were finalized by studying their respective concentrations in the human serum. Fig. 5A shows that negligible changes in the current signal (3.5%, 0.4%, 1.9%, 1.5% and 3.9%) were detected after the addition of Chol, urea, TB, AA, and UA, respectively. These results indicated that the presence of interferents in the serum barely affected the process of glucose detection. Thus, the GOx/NPG/GCE bioelectrode showed a strong anti-interference capability during the practical determination of glucose in serum samples.

3.6. Determination of glucose in human serum samples

The practical performance of the GOx/NPG/GCE bioelectrode was tested by detecting the glucose concentration in human serum. A rapid and stable response current density value was acquired at +0.3 V. By substituting the value into the calibration curve, the concentration of glucose in the human serum sample was calculated. The obtained results are shown in Fig. 5B. The results were compared with those obtained by an automatic biochemical analyzer, and the data obtained from the two devices were in good agreement. This result demonstrated that the as-prepared biosensor was practical and effective for the determination of glucose in actual human serum samples.

4. Conclusion

In summary, the GOx/NPG/GCE bioelectrode was successfully fabricated by encapsulating GOx onto NPG with a three-

A

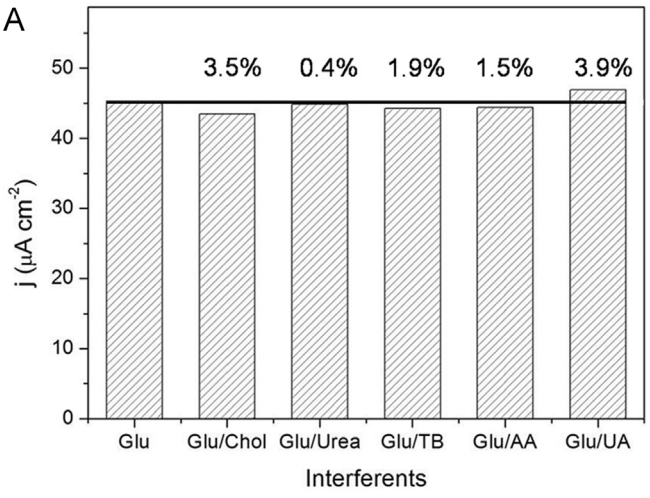

B

Sample no.	Concentrations of glucose (mM)		Deviation rate (%)
	Determined by GOx/NPG/GCE bioelectrode (mM)	Determined by automatic biochemical analyzer (mM)	
1	6.0	6.2	3.3
2	4.7	4.6	2.2
3	5.6	5.3	5.4
4	6.5	6.2	4.6

Fig. 5. Effects of interferents on the GOx/NPG/GCE bioelectrode (A). Comparison between the concentrations of the glucose measured with the GOx/NPG/GCE bioelectrode and with the automatic biochemical analyzer (B).

dimensional nanoporous structure, thus providing a good interface between the active sites of enzyme and the underlying electrode. The efficient electrocatalytic oxidation of glucose on the surface of the resulting GOx/NPG/GCE bioelectrode was completed by the interaction of GOx and NPG, thus offering excellent sensing performance with high sensitivity, anti-interference ability, and good stability. Additionally, the GOx/NPG/GCE bioelectrode also presented reliable detection for glucose in human serum samples.

Acknowledgments

This work was supported by Grants from the National Natural Science Foundation of China (21177074), Science and Technology Fund Planning Project of Shandong Province, China (2014GSF117021), New Teacher Foundation of Ministry of Education of China (20090131120005), and Distinguished Middle-Aged and Young Scientist Encourage and Reward Foundation of Shandong Province, China (BS2010SW016).

Appendix A. Supplementary information

Supplementary data associated with this article can be found in the online version at http://dx.doi.org/10.1016/j.bios.2014.11.037.

References

Chang, G., Shu, H., Ji, K., Oyama, M., Liu, X., He, Y., 2014. Appl. Surf. Sci. 288, 524–529.
Clark jr., L.C., Lyons, C., 1962. Ann. N. Y. Acad. Sci. 102, 29–45.
Ding, Y., Chen, M., 2009. MRS Bull. 34, 569–576.
Ding, Y., Kim, Y., Erlebacher, J., 2004. Adv. Mater. 16, 1897–1900.
El-Daeb, M.S., Ohsaka, T., 2002. Electrochim. Acta 47, 4255–4261.
Fu, Y., Liang, F., Tian, H., Hu, J., 2014. Electrochim. Acta 120, 314–318.
Gao, Y., Yang, T., Yang, X., Zhang, Y., Xiao, B., Hong, J., Sheibani, N., Ghourchian, H., Hong, T., Moosavi-Movahedi, A.A., 2014. Biosens. Bioelectron. 60, 30–34.
Gu, H., Yu, Y., Liu, X., Ni, B., Zhou, T., Shi, G., 2012. Biosens. Bioelectron. 32, 118–126.
Hecht, H.J., Schomburg, D., 1993. Biosens. Bioelectron. 8, 197–203.
Heller, A., Feldman, B., 2008. Chem. Rev. 108, 2482–2505.
Hsu, C., Wang, G., 2014. Biosens. Bioelectron. 56, 204–209.
Hudson, S., Cooney, J., Magner, E., 2008. Angew. Chem. Int. Ed. 47, 8582–8594.
Jiang, L., Liu, H., Liu, J., Yang, Q., Cai, X., 2008. J. Electroanal. Chem. 619–620, 11–16.
Laviron, E., 1979. J. Electroanal. Chem. 100, 263–270.
Liu, Z., Huang, L., Zhang, L., Ma, H., Ding, Y., 2009. Electrochim. Acta 54, 7286–7293.
Qiu, C., Wang, X., Liu, X., Hou, S., Ma, H., 2012. Electrochim. Acta 47, 140–146.
Ravindra, R., Zhao, S., Gies, H., Winter, R., 2004. J. Am. Chem. Soc. 126, 12224–12225.
Scanlon, M., Salaj-Kosla, U., Belochapkine, S., MacAodha, D., Leech, D., Ding, Y., Magner, E., 2012. Langmuir 28, 2251–2261.
Solanki, P.R., Dhand, C., Kaushik, A., Ansari, A.A., Sood, K.N., Malhotra, B.D., 2009. Sens. Actuators B: Chem. 141, 551–556.
Sotiropoulou, S., Vamvakaki, V., Chaniotakis, N.A., 2005. Biosens. Bioelectron. 20, 1674–1679.
Vijayalakshmi, A., Tarunashree, Y., Baruwati, B., Manorama, S.V., Narayana, B.L., Johnson, R.E.C., Rao, N.M., 2008. Biosens. Bioelectron. 23, 1708–1714.
Wang, X., Liu, X., Yan, X., Zhao, P., Ding, Y., Xu, P., 2011. PLoS One 6, e24207.
Wei, C., Li, X., Xu, F., Tan, H., Li, Z., Sun, L., Song, Y., 2014. Anal. Methods 6, 1550–1557.
Wu, C., Liu, X., Li, Y., Du, X., Wang, X., Xu, P., 2014. Biosens. Bioelectron. 53, 26–30.
Yan, X., Meng, F., Xie, Y., Liu, J., Ding, Y., 2012. Sci. Rep. 2, 941.
Zhang, S., Wang, N., Niu, Y., Sun, C., 2005. Sens. Actuators B: Chem. 109, 367–374.
Zhang, X., Ding, Y., 2013. Catal. Sci. Technol. 3, 2862–2868.